SCIPP 04/04

University of California
Santa Cruz

Silicon Strip Detector Efficiency Using a Purpose Built Particle Telescope

This report is funded by Crown Fellowship
and conducted at Santa Cruz Institute for Particle Physics

By

John Wray, UCSC Senior

May 2004

Abstract:

Ionizing particles are used in many fields: astrophysics, physics, chemistry, biology, and medicine just to name a few. At SCIPP we are continually developing new detection systems to track particles such as: photons, protons, and electrons based on semiconductor ("Silicon Valley") technology. One parameter of great importance to the tracking system is the efficiency of the detectors. We have developed and built a concise system to measure the efficiency of Silicon Strip detectors with a radioactive source. The operation and performance of the "particle telescope" is described. During the design phase, a deeper insight into the beta spectrum of the radiation source was required, which led me to a understanding of the theory of nuclear beta decay of Enrico Fermi.

Table of Contents:

1. Introduction:

The goal of this research paper is to build a custom particle telescope and to use this telescope to determine the detection efficiency of Silicon Strip Detectors (SSD). As in any validation experiment, we must first normalize the operation of the tools. In our case, we are using a scintillator coupled to a photomultiplier tube (PMT) to validate the detection of particles passing through the SSD.

Determining the efficiency of the SSD setup will involve the analyzing of two sets of data. One set of data coming from the Silicon Strip Detector, the other coming from the scintillator. Analysis will be done using electronic components like discriminators, Logic Modules, Gate Generators, Frequency Counters, and specifically designed programs to automate data collection.

A background chapter has been included, which will offer some explanation of radiation length used in the measurement of the beta decay energy spectrum. This experiment relies on the use of a PMT and SSD to capture beta counts. So, A description of the fundamental operation of the PMT and SSD has been included.

The Examples of SSD Application chapter is included to offer a view into the world of SSD application. This chapter also offers a place to describe the application of the SSDs that are being tested for efficiency of particle counting.

In the Materials and Experimental Methods chapter I will provide a list of research equipment. The concept for, and construction of the particle telescope will be discussed in this chapter. The Operational Parameters of the PMT chapter will talk about how the PMT was setup and give some count rates data collected during the verification process. The Efficiency Setup chapter will offer diagrams and actual pictures of the experimental setup. This chapter will also serve as a place to describe how the efficiency of the SSD will be calculated.

The finial two chapters will be use to offer the results of this experiment and give some conclusions. In the Appendix there will be more pictures of the efficiency setup, and some mechanical drawings of the collimator.

2. Background:

2.1 Energy Loss of Electrons in Matter:

It is well known that ionized particles lose energy as the particle travels through matter. High-energy electrons predominantly lose energy in matter by bremsstrahlung. The amount of energy loss in matter is characterized by what is commonly referred to as radiation length. It is the mean distance over which a high-energy electron loses all but 1/e of its energy due to bremsstrahlung.

At low energies electrons primarily lose energy by ionization, though other processes do contribute. The loss of energy by an electron is dominated by bremsstrahlung above a few tenths of a MeV in most material.

During this experiment the beta energy spectrum was measured. When finding the beta spectrum the energy loss over the path length must be accounted for to accurately calculate beta spectrum. The experimental beta spectrum was measured through approximately 2.94 cm of air and 1.5 mm of paper tape and Mylar, which covers the scintillator.

Information on electron energy loss in materials is available through the National Institute of Standards and Technology (NIST) ESTAR database. Figure 1 is a composite graph that was created so that approximates energy loss predications could be made. To calculate the radiation length the maximum energy on the x-axis was found. The density of the material then multiplied the corresponding y-axis value. From the graph below it was concluded that the Strontium-90 (Sr-90) beta particle would not make it though 2.94 cm of air and 1.5 mm of tape & Mylar, where the Yttrium-90 (Y-90) betas will lose ~500 keV in 2.94 cm of air and 1.5 mm of tape & Mylar.

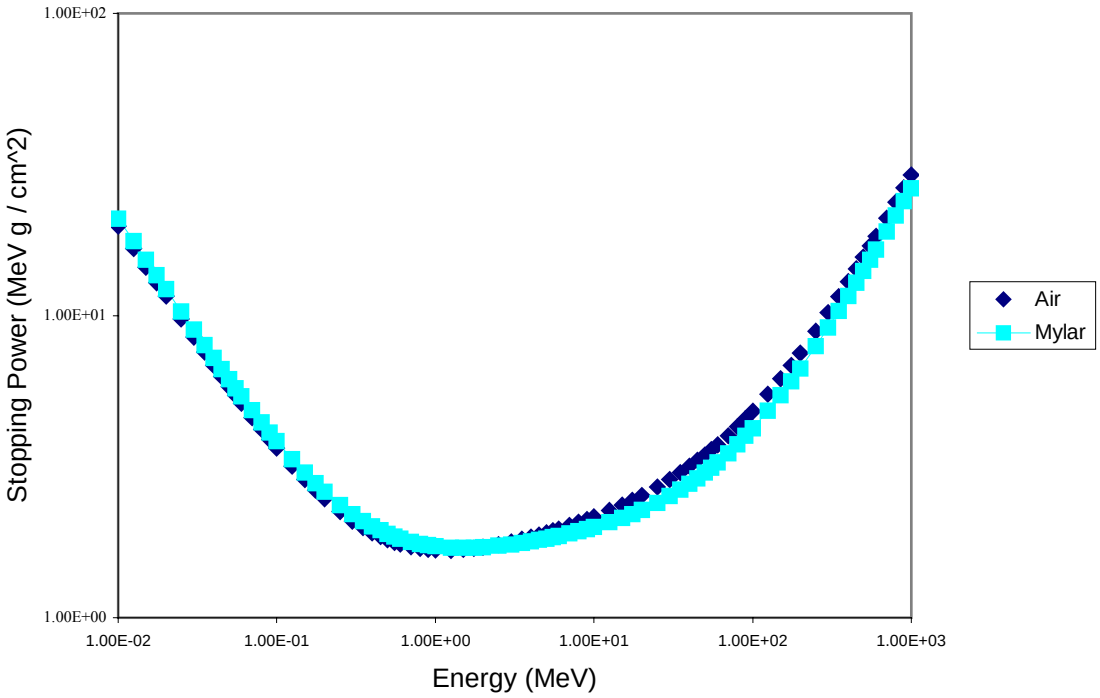

Figure 1: Radiation Length [1]

2.2 Scintillation Counter and Photomultiplier Tube (PMT):

The scintillator, light guide, and photomultiplier tube work in conjunction to act as a particle detector. The diagram below outlines the internal components.

The light shield of our scintillator is black tape, which was verified to not let any light penetrate to the scintillator. This was done by operating the scintillator, light guide and PMT with and without a covering of heavy black felt. The counts from both types of operation are within standard statistical error of each other. The PMT consists of an evacuated glass tube, dynodes, anodes and electrical components.

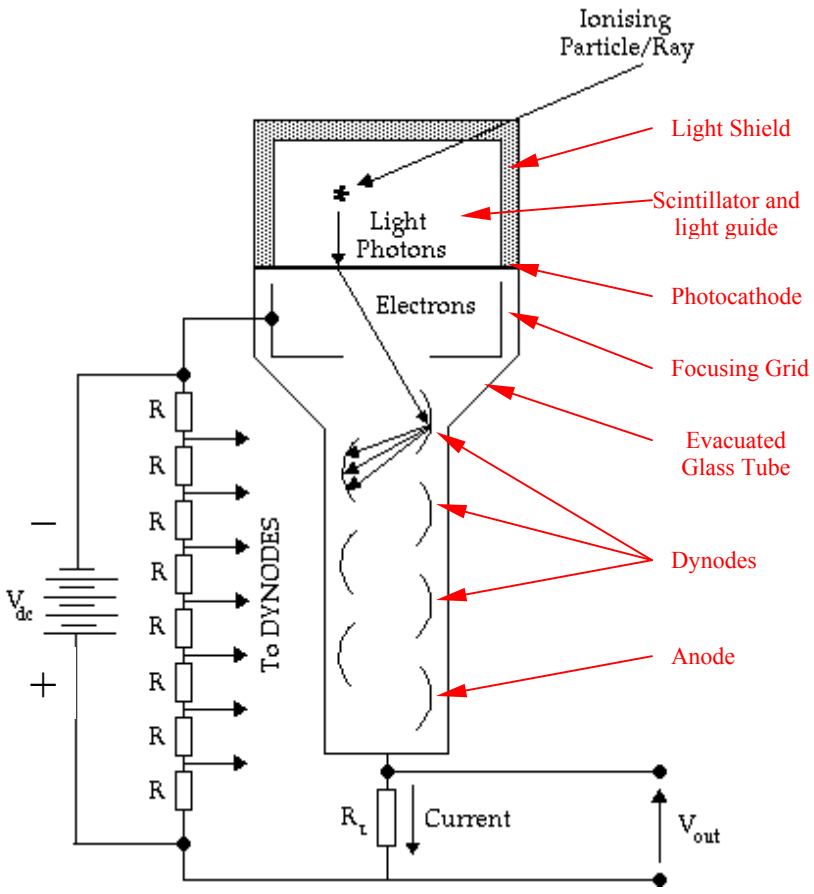

Figure 2: PMT functional diagram [2]

The PMT is operated with a negative voltage polarity in the kilovolt range. Figure 3 shows a schematic overview of what happens when an incident particle impacts an atom of the scintillator, and excites a valance electron. For this electron to return to its lowest energy state, a photon must be emitted. This photon travels down the light guide impacting the photocathode producing a photoelectron inside the PMT. This photoelectron is accelerated toward the leading dynode where multiple electrons are produced and accelerated toward the next dynode in the chain. This process is repeated several times. The resulting electrons impact the anode generating an electrical pulse [3]. This electrical pulse is passed to a discriminator, which returns a Nuclear Instruments Module (NIM) pulse for every signal received from the PMT over a settable threshold voltage. The NIM pulse is sent to a counter to determine the counting rate, or other logic module for signal processing.

2.3 Silicon Strip Detectors (SSD):

The SSD begins with a basic substrate of pure crystal silicon that is doped with n-type impurities on one side and p-type on the other. P-type strips are implanted in the silicon and then covered with thin strips of aluminum. The bottom is uniformly covered with a layer of n-type and then aluminum.

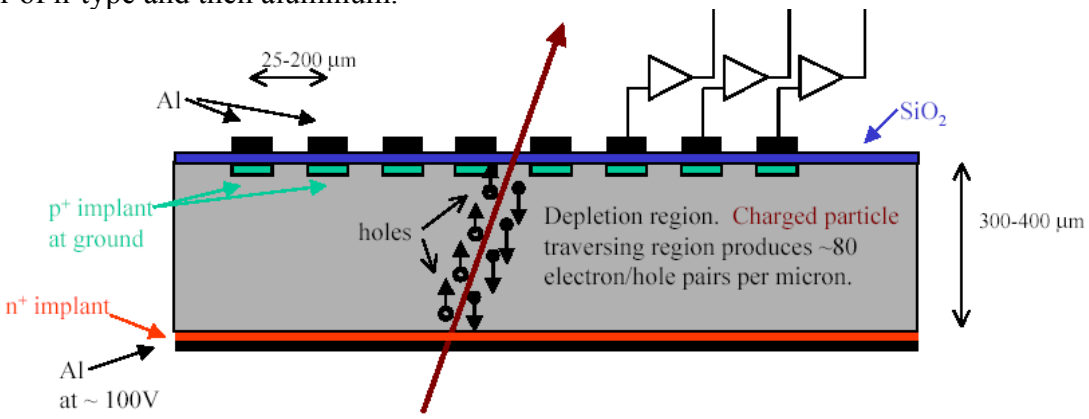

Figure 3: Diagram of a single-sided silicon strip detector [5]

With no bias voltage applied there is a natural mutual attraction between the free electrons from the n-type impurities and the free holes from the p-type. This attraction creates a region in the bulk of the substrate called a depleted region. A bias voltage is applied to the SSD in order to enhance the depleted region. It is in this enhanced depleted region where particle detection takes place.

When a particle passes through the depleted region in the silicon, ionization occurs. The ionization of the silicon atoms causes the valence electron to move into the conduction band. The conduction electron is then attracted to the ground plate at the bottom of the detector. An electric field is set up between the silicon ions and the positively biased aluminum strips, the electric field causes a conduction electron from the aluminum to drift to the silicon ion. The departing aluminum conduction electron causes a current to flow from the particular strip. The current supplies the silicon atom with electrons to deionize and return the surrounding region to a depleted state.

In the readout electronics the current is amplified and translated in to a digital signal. The digital signal is recorded and analyzed in two ways: the time the current is over the threshold current, and the strip address. The time over threshold tells us the energy deposited. The strip address tells us the position where the particle passed through the detector. These two sets of data give a very detailed picture of the particles position and energy.

3. Examples of SSD Application:

3.1 Proton Tracking Silicon Microscope (PTSM):

The picture below is the main read out controller for the PTSM project, the SSD is not mounted in this picture instead there are capacitors that are used for calibration.

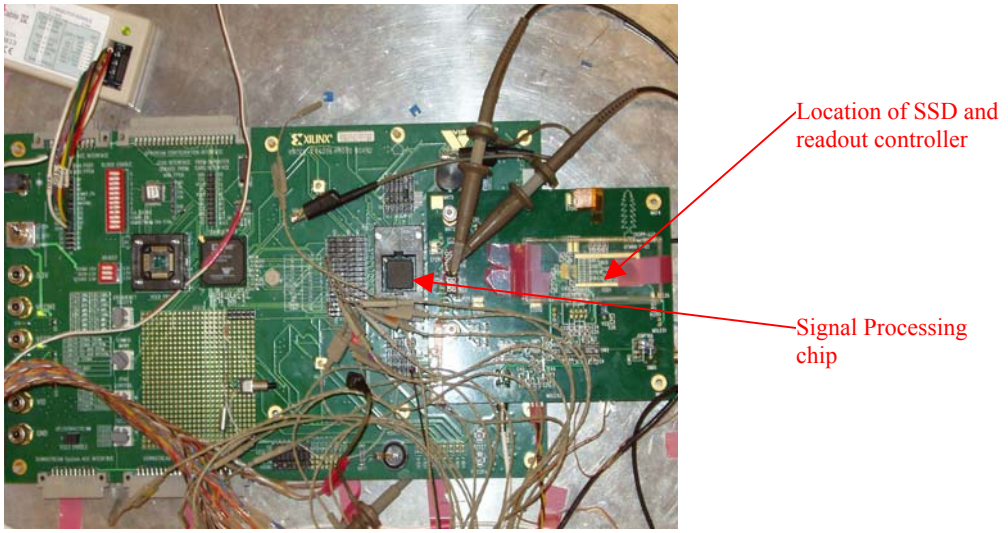

Figure 4: PTSM in development

The goal of the PTSM project is to measure the energy deposited in biological material. Theoretically, with the initial momentum of the particle and the densities the particle went through the energy deposition can be measured [4]. A set of orthogonal SSDs will allow the precise determination of trajectory.

The PTSM project uses the position and energy loss of the proton and/or heavy ion as a form of very precise molecular imaging. The reason heavy ions are used is due to the very sharp Bragg peak. They deposit their energy in a very small region after a certain amount of the initial energy loss. For the purposes of PTSM the proton is given enough energy so that the Bragg's peak will be after particle detection. The minimal amount of energy loss will allow a very precise calculation of the exact densities the particle passed through.

3.2 Nanodosimetry (ND):

The Nanodosimetry project uses single ion counting to understand basic ionizing radiation interactions on the molecular level. The experimental setup of the ND project begins with two pairs of single-sided SSDs placed at right angles to each other, one set in front of the ion counter and one behind.

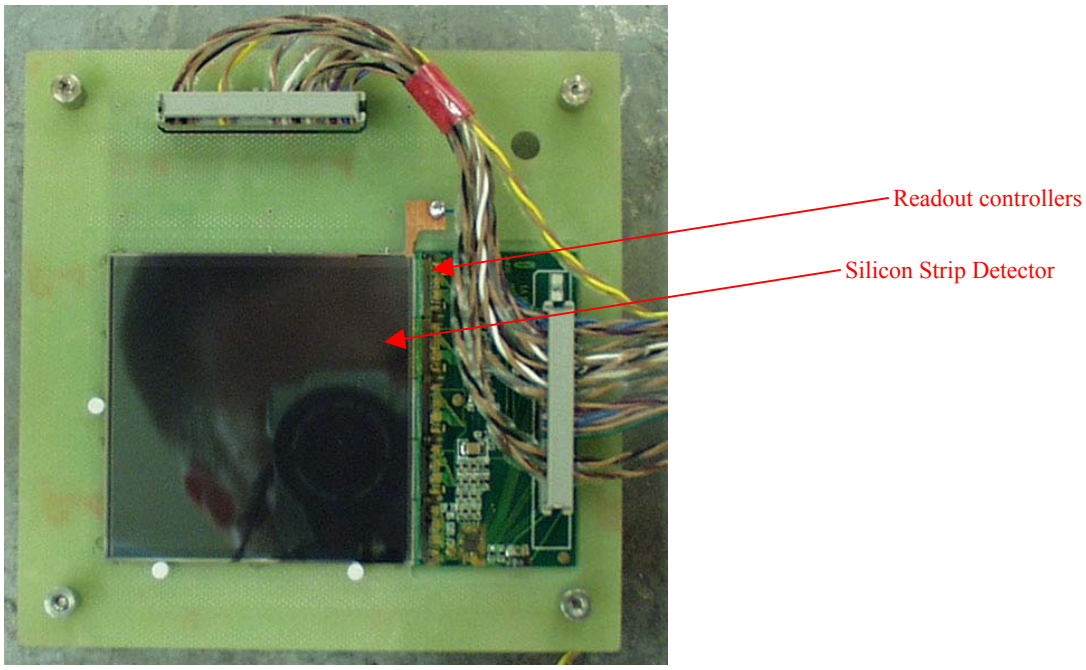

Figure 5: One set of SSDs for the ND project [6]

The ND project uses low-pressure propane gas to model DNA segments. The ND project is trying to study the effects that ionizing radiation has on the DNA structure and what the effects are of a single strand break and a double strand break.

The study begins with a beam of protons. The initial position and energy of the protons are measured by the first set of SSDs. The proton then passes through the propane where the proton breaks the propane chains into other chemical compounds. Finally the protons pass through the second set of SSDs. The two sets of SSDs are used to determination of the proton energy loss, and constrain the particle trajectory to the active region of the apparatus.

4. Materials and Experimental Method:

The experiments to measure the efficiency of detectors used the following equipment: Particle Telescope, Mounting Stage, High Voltage Power Supply, Scintillator/Light Guide, PMT, ND SSD Module, PTSM SSD Module, Discriminator, Gate Generator, Frequency Counter, Coincidence Module, Semiconductor Parameter Analyzer, DC Power Supply, AC Power Supply, Oscilloscope, Strontium-90 radiation source, customized Nanodosimetry software, customized PTSM software, and a Light Box.

4.1 Particle Telescope:

The concept of the particle telescope is to have a radiation source positioned over a SSD and a PMT. The radiation will pass through the SSDs first then the PMT as diagramed in Figure 7.

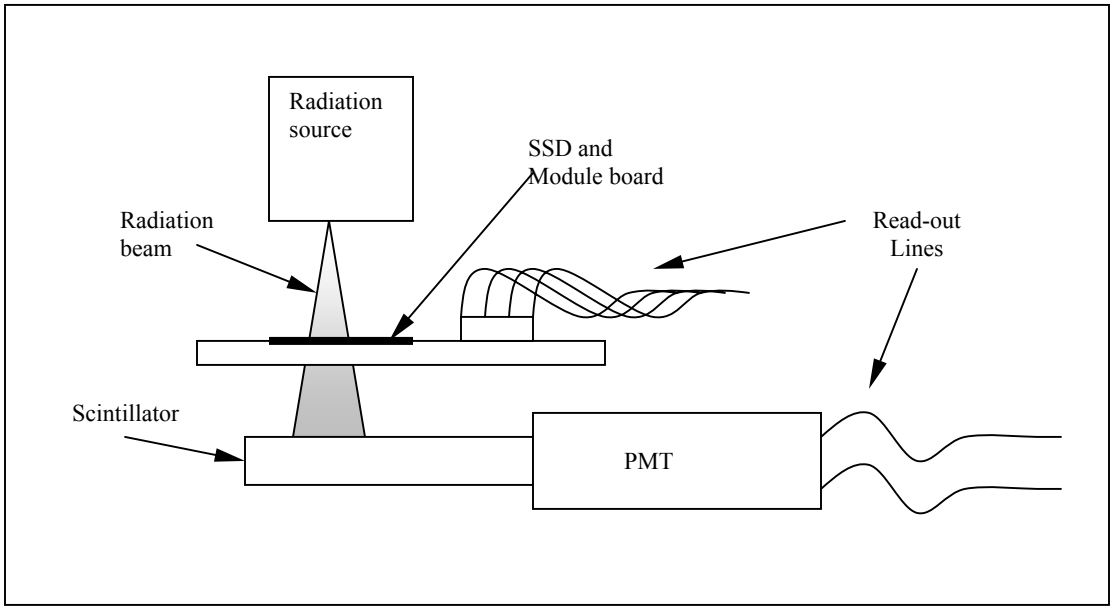

Figure 6: Diagram of SSD and PMT setup

The construction of the particle telescope begins on a micro-position base. The function of this base will allow the precise movement of the particle telescope over the SSD being studied. The base can move in both transverse directions with increments of one micrometer. On top of the micro-position base a platform will support the PMT and collimator. The platform is made out of 5051 aluminum, which is attached to the micro-position base by four countersunk screws.

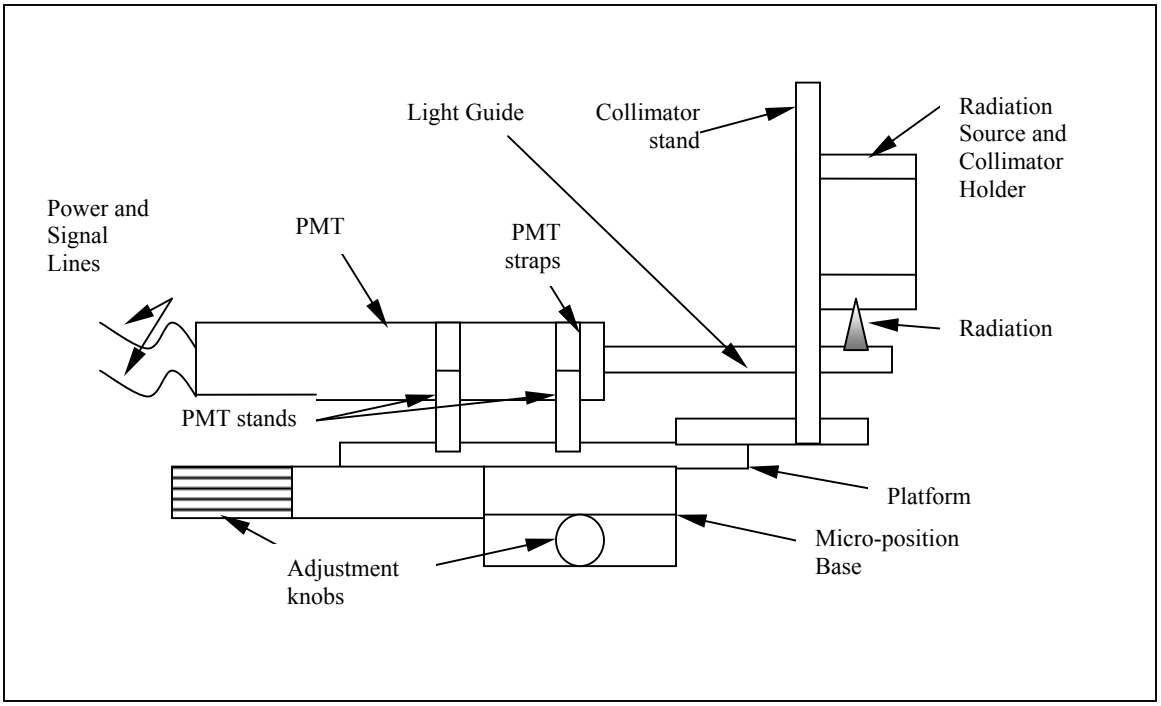

Figure 7: Diagram of the Particle Telescope

A container was made to hold the radiation source, and a ⅜" thick brass collimator in perfect alignment.

The walls of the container was constructed out of a 3" cylinder of 5051 aluminum with ¼" walls. Notches were cut into the top and bottom of the cylinder to create room for press fit caps.

Both caps were constructed out of 5051 aluminum. The top cap was made ⅜" thick, and to perfectly fit inside the cylinder. The bottom cap needed a special recess area for the collimator, along with a slit to expose the collimated radiation to the object.

The stand was inspired by a chemistry stand. It was constructed out of 5051 aluminum. The upright was made out of ½" bar, and the base was made of ½" x 2.5" x 4" plate. The upright was threaded and the base was tapped so the two pieces screw together. The stand is attached to the platform by four countersunk screws. The PMT stands were also made out of 5051 aluminum, using screw straps to attach the PMT to the stands. The PMT stands were attached to the platform using two screws per stand. The pieces of the collimator holder are diagramed in Appendix A3.

4.2 Operating Parameters of the PMT:

The first order of business was setting up all the electrical components. This was done as in Figure 11. To determine if the scintillator, light guide, and PMT were in working order, I supplied power to the PMT. With no radiation source present the noise of the PMT and cosmic background radiation was measured.

The noise was measured by scanning the threshold from –50 to –1000 mV. These threshold scans were done for supply voltage of 1700, 1800, 1900, 2000 volts. For decent statistics ten sets of ten second counts were taken, and the average reported.

In order to understand the operating parameters of the PMT, the collimated Strontium-90 radiation source was placed ~2.94 centimeters above the scintillator. Scanning the threshold voltages for each of the four high voltage supplies gave a data set that could be analyzed into the following graphs. All of the data was collected in a low/no light condition to rule out any counts from light.

4.2.1 PMT Readout Electronics

To readout the count rates for the beta spectrum a series of electronic components had to be put together. The signal that comes out of the PMT was very weak and had a very short duration. Therefore this signal was passed to discriminator, which put out a healthy NIM pulse. The resulting NIM pulse can be passed to a frequency counter, which will recognize this as a trigger signal. Custom software was designed to readout the frequency counter and input the data into an Excel spreadsheet. The program code that was used to readout our frequency generator is available in Appendix A4.

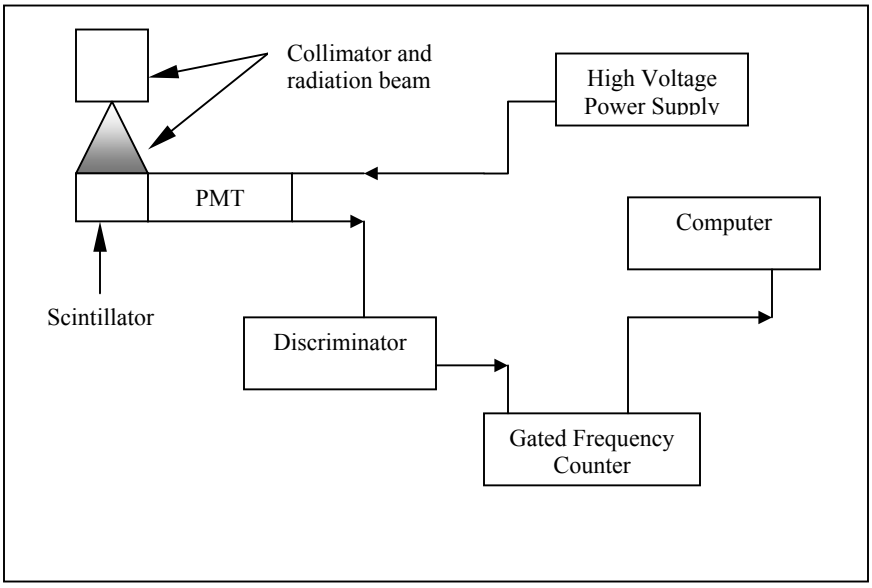

Figure 8: Schematic of the PMT readout electronics setup

4.2.2 Plateau Curve:

The plateau curve is used to determine the optimum input voltage. The PMT counts most efficiently in the region where the graph has an inflection point. By looking for a common inflection point in all five threshold curves, it can be seen that -1800 volts is an efficient operating voltage.

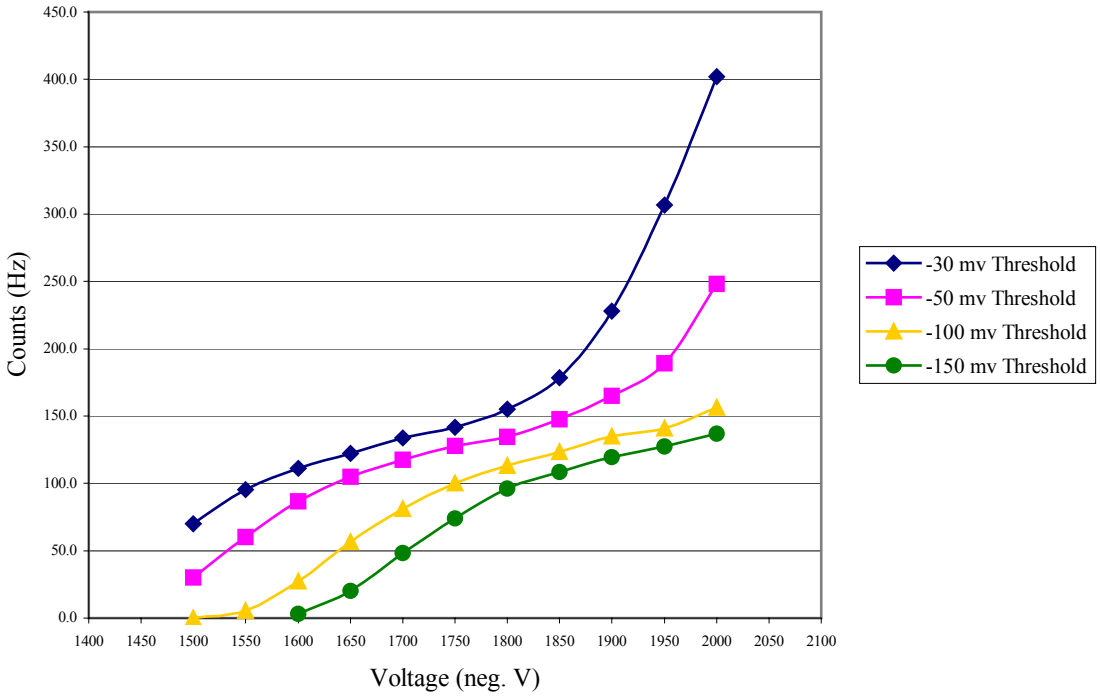

Figure 9: Plateau Curve

4.2.3 Noise and Counts Curve:

The noise of the PMT tell us under what conditions the count rates can not be trusted due to excessive error. We are looking for a threshold voltage that will be out of the noisy region and still give us a reasonable counting rate. From Figure 10, it can be seen that there is less noise for higher threshold voltages. Counts curve are useful to give a relationship between the number of counts and the threshold voltages. In Figure 10 the noise was subtracted out of the counts curve.

Common sense suggests that at zero millivolts threshold there will be one hundred percent counting efficiency. Using this line of thinking, I plotted (counts – noise) vs. threshold. This gave the following equation:

$$y = (3\times10^{-14})x^6 - (7\times10^{-11})x^5 + (6\times10^{-8})x^4 - (3\times10^{-5})x^3 + 0.0055x^2 - 1.2018x + 267.58$$

with an R^2 value of 0.9997, which allowed an approximation for the maximum counting rate. I used, maximum counting rate = 100% counts, to calculated a conversion factor between percent and counts, 1 ct = 0.373134 %. I used this to conversion to create the following graph. I also used this conversion on the noise. In the counts graph if have included the error which is the square root of the counts, which was then converted in to a percent using the conversion factor.

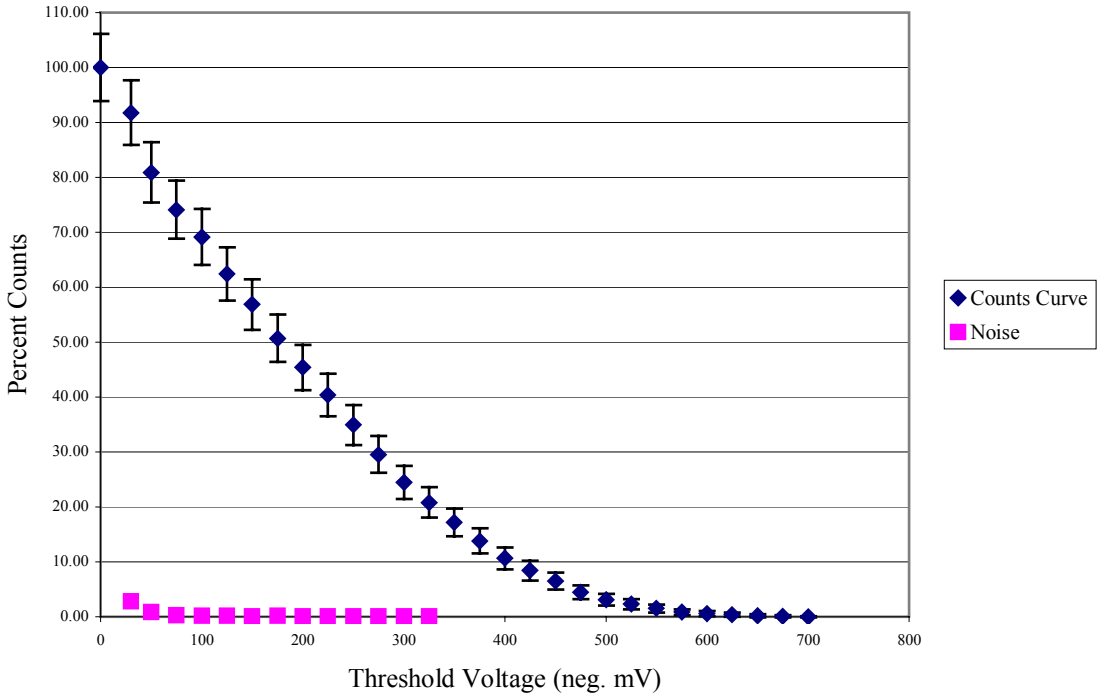

Figure 10: Percent Counts and Noise vs. Threshold Voltage

4.3 Efficiency setup:

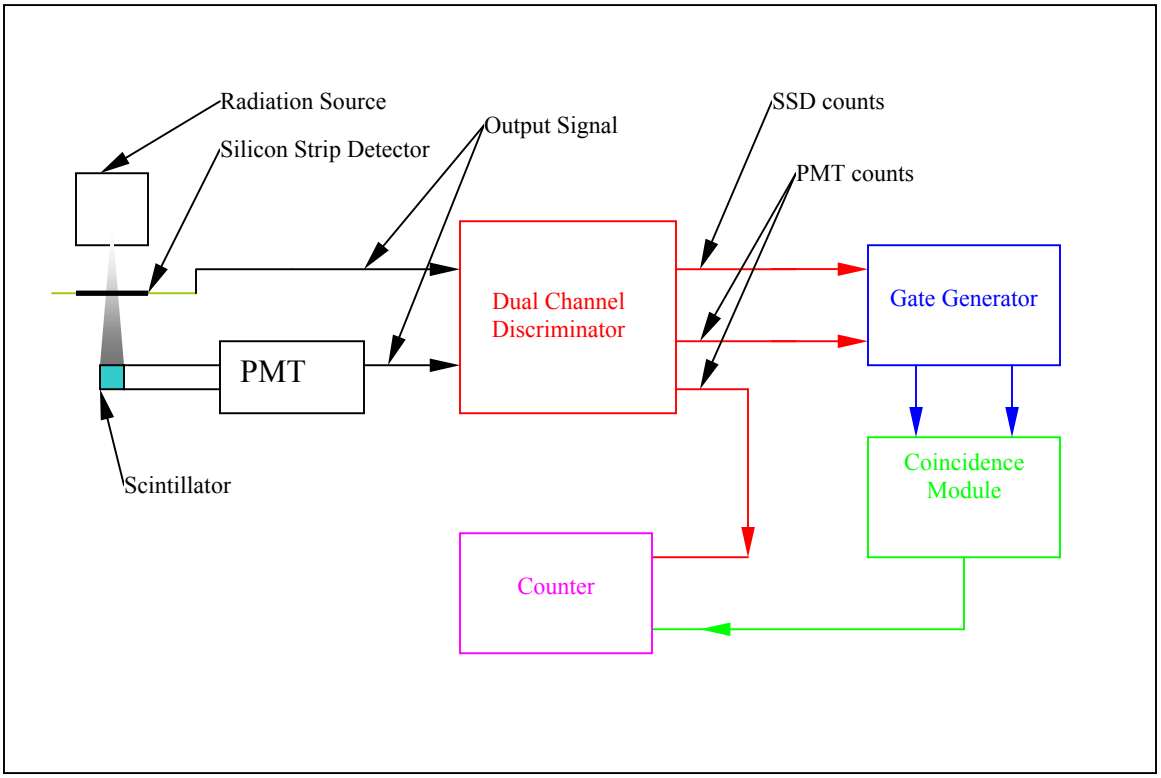

Figure 11: Experimental Efficiency Setup

The radiation source, SSD and scintillator are located in a black box, which excludes any counts from light. the ND SSDs will be checked for efficiency in a black box. The experiment to determine the efficiency will use the Scintillator and the bottom SSD of the ND setup. The efficiency will be calculated from ratio of the coincidence of the PMT and the bottom SSD vs. (PMT – PMT noise) counts.

The SSDs is inherently very low noise so a reasonable threshold on each setup will remove any unwanted noise counts. All counts will be collected at the same time in one and a half hour time segment.

5. Results:

5.1 Energy Spectrum of Beta Decay:

The information about electron energy loss in air described in section 2.1 will be used to make energy spectrum corrections. During the investigation into the SSD counting efficiency it became apparent that the scintillator counting rate spectrum was the integral of the pulse height spectrum. Thus, the energy spectrum of beta decay can be determined from differentiating a fit equation from the data collected. With this calculated experimental energy spectrum we can confirm Enrico Fermi's theory of weakly interacting beta decay. The energy spectrum from Fermi's theory is well known and the plot is generally a function of energy density of finial states verses particle energy.

In this experiment we are using a Strontium-90 source. Strontium-90 has a short-lived daughter isotope of Yttrium-90. Each of these radioactive isotopes has maximum beta decay energy, 0.546 and 2.283 MeV respectively [7]. Shown in Figure 13 is the decay of Strontium-90 along with the second and tertiary products.

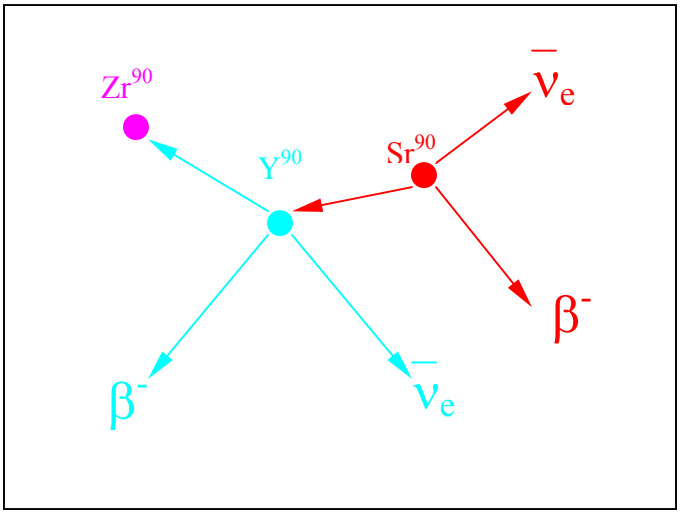

Figure 12: Diagram of Beta Decay and resulting isotopes

The experimental energy spectrum of beta decay can be calculated by fitting a curve to the count rate spectrum. Setting the maximum threshold to the maximum beta energy, taking in consideration the loss of particle energy due to the travel in air, will give us a conversion factor, 1 mV = 0.003675 MeV. Using the conversion between threshold and energy I created a graph of counts verse particle energy. Differentiating the count rate fit equation produced the experimental energy spectrum of the Strontium-90 + Yttrium-90 source. The theoretical energy spectrum is thanks to Enrico Fermi and his studies of weak interaction forces. The resulting theoretical equation is the energy density of finial state as a function of particle momentum. The equation is commonly given as [8]

$$N(p)dp \propto p^2 (E_o - E)^2 \, dp$$

were the neutrino is considered mass-less and that the beta particles are relativistic, and therefore its momentum is given by:

$$p^2 = E_f^2 - m^2$$

$$E_f = E_i + m$$

The E_f in the invariant momentum relation pertains to the energy of the particle after pair creation, the E_i is the particle energy before pair creation and m in both equations is the rest energy of the beta particle. The lack of the speed of light constant this is because I have used natural units such that the speed of light is one. Considering the above equations allows the energy density to be a function solely of energy. The use of conversion factors allowed me to scale the theoretical predictions to fit the experimental results. In order to match the theoretical beta decay spectrum to the experimental spectrum energy cuts had to be made using the approximations in chapter 2.1. Figure 13 shows the complete theoretical beta decay spectrum. In Figure 14, 15, and 16 show how the energy cuts made the difference between a terrible match and an excellently matched spectrum.

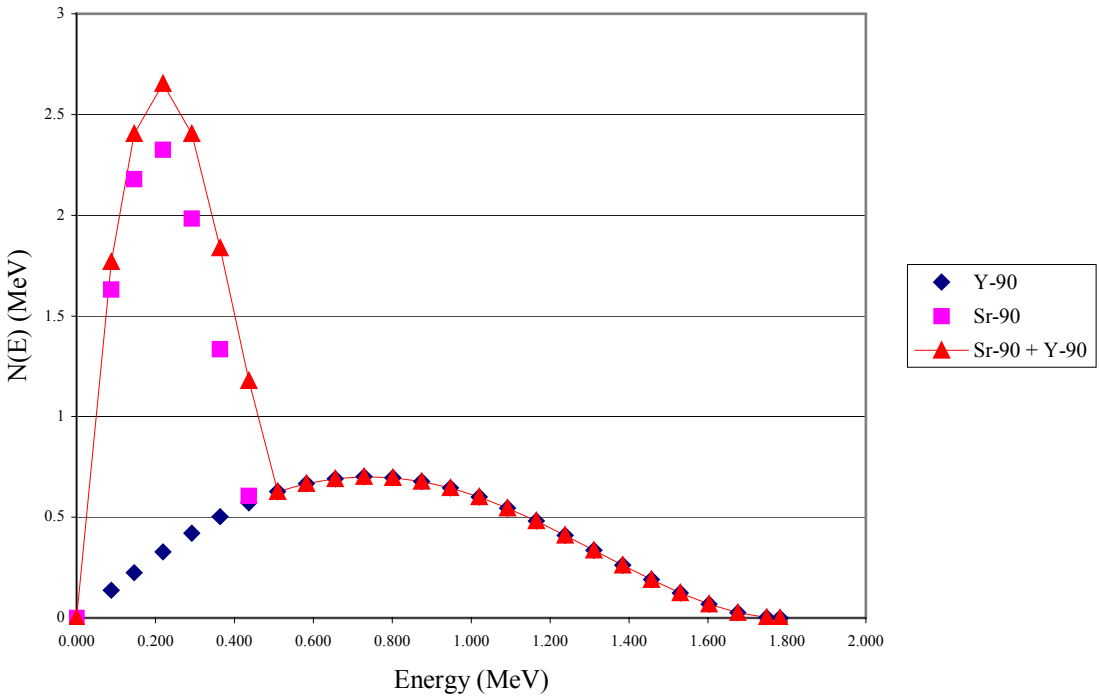

Figure 13: Theoretical Composite Energy Spectrum

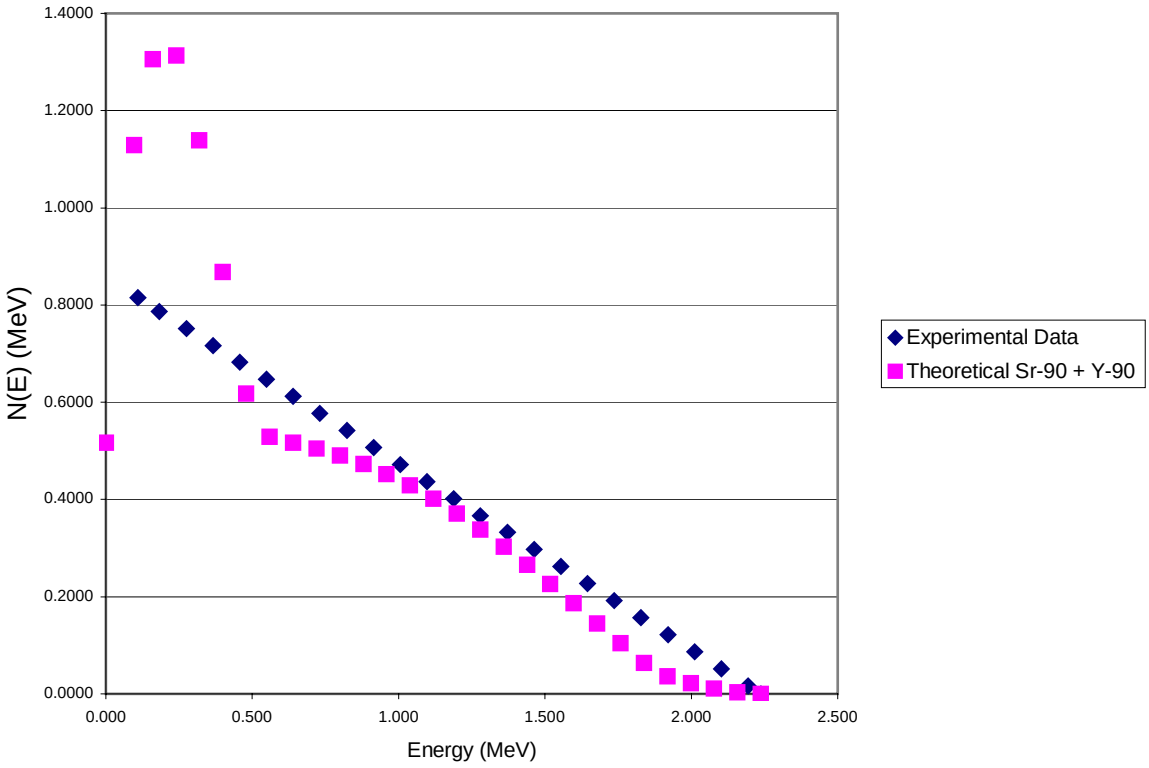

Figure14: Theoretical and Experimental Spectrums with no energy cuts

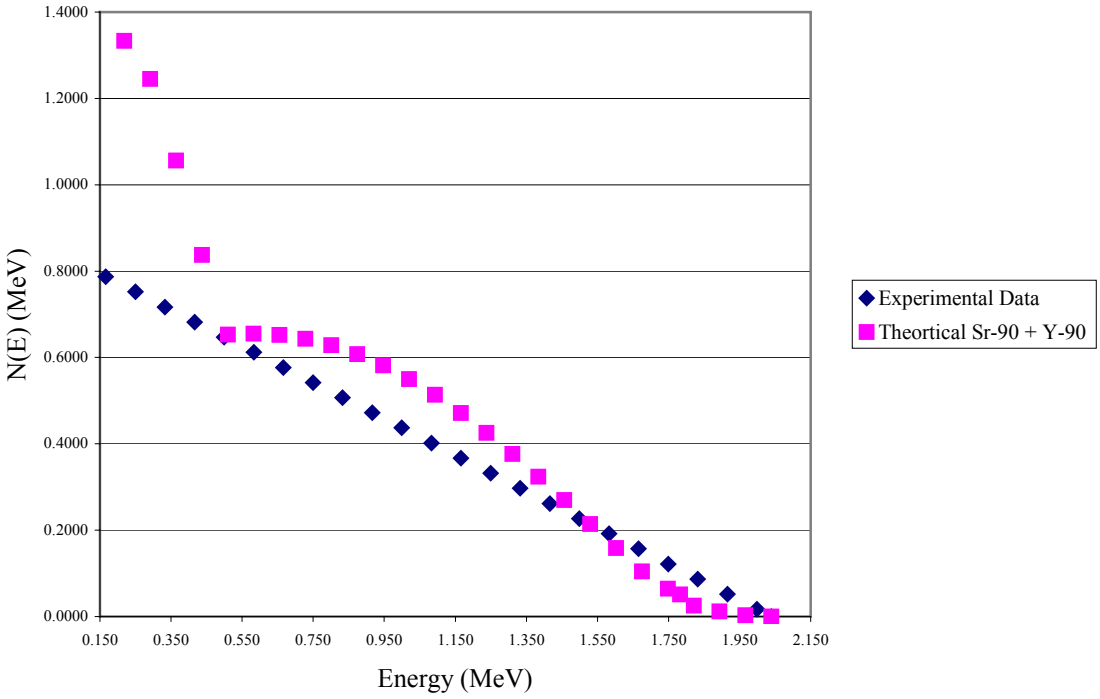

Figure 15: Theoretical and Experimental Spectrums with cuts for energy loss in air

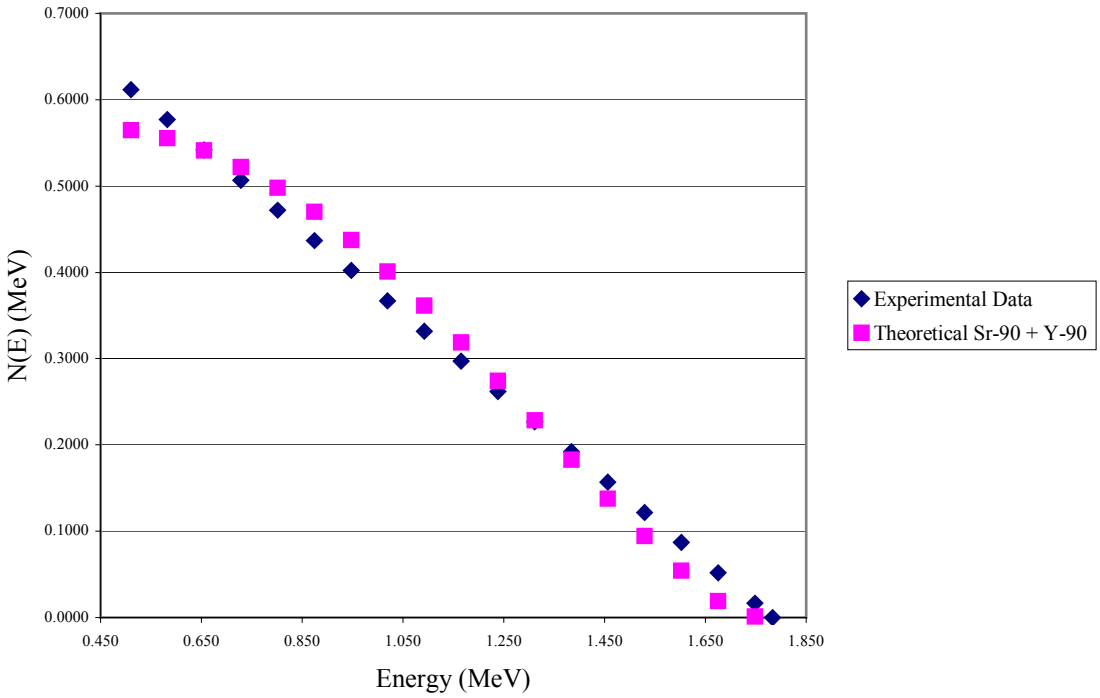

Figure 16: Theoretical and Experimental Spectrums with energy cuts for air and Mylar

5.2 Efficiency of SSD:

For our situation the only way to reduce the amount of uncertainty was to run the experiment for extended time period in order to build up counts. The error of the experiment is give by the expression:

$$\sigma_{\varepsilon}^2 = \left(\frac{\partial \varepsilon}{\partial N_{trg}}\right)^2 \sigma_N^2 + \left(\frac{\partial \varepsilon}{\partial m}\right)^2 \sigma_m^2$$

The 'σ' terms are the variance, the subscript indicates efficiency, missed counts, or scintillator counts. 'ε' is the efficiency of the experiment. 'm' is the difference in number of counts between the scintillator and the SSD. 'N' is the number of counts, the subscript denotes scintillator (trg) or coincidence (con). The error for the two experimental efficiency setups will have to be calculated separately. The equations for the efficiency, 'ε', and the difference in counts, 'm', are give by:

$$\varepsilon = 1 - \frac{m}{N_{trg}}$$

$$m = N_{trg} - N_{con} = (1-\varepsilon)N_{trg}$$

The uncertainty or percent error of the efficiency is given by:

$$\frac{\sigma_\varepsilon}{\varepsilon} = \sqrt{\frac{m}{N_{trg}^2}\left(1-\frac{m}{N_{trg}}\right)^2}$$

There are two limiting cases in determing the percent error.

For the first limiting case when: $\frac{m}{N_{trg}} \approx 1$ the percent error is given by:

$$\frac{\sigma_\varepsilon}{\varepsilon} = \sqrt{\frac{m}{N_{trg}^2} - \frac{2m}{N_{trg}}}$$

For the second limiting case: $\frac{m}{N_{trg}} << 1$ the percent error is given by:

$$\frac{\sigma_\varepsilon}{\varepsilon} = \sqrt{\frac{m}{N_{trg}^2}}$$

Efficiency data of ND setup:

	Total Number of counts
PMT & Lower SSD	106445
PMT	109371
PMT noise	2298

$$\varepsilon_{ND} = 1 - \frac{(109371-2298)-106445}{(109371-2298)} = 99.4\%$$

With bounding errors of:

$$\frac{\sigma_\varepsilon}{\varepsilon} = \sqrt{\frac{m}{N_{trg}^2} - \frac{2m}{N_{trg}}} = 0.108\% \qquad \frac{\sigma_\varepsilon}{\varepsilon} = \sqrt{\frac{m}{N_{trg}^2}} = 0.077\%$$

During the each experiment the light conditions would be considered very low inside the sensitive region. Three layers of black felt covered the light box containing the efficiency setup.

6. Conclusions:

Particle Telescope:

The particle telescope was designed and constructed to be useful in future experiments. The overall performance of the telescope in this experiment has been excellent. The telescope allowed the source and PMT to stay in perfect alignment while the micropositioner made it possible to test different areas of the SSD. The ability to change the distance between the PMT and the radiation source was extremely useful.

Future upgrades to the particle telescope could include another attachment point for a second PMT. Height adjustment for the PMT would be a useful enhancement. The platform for the micropositioner could be reduced in size to take up less table space. A freestanding height adjustable general testing platform needs to be developed.

Energy Spectrum of Beta Decay:

There was great excitement when graphs in Figure 14 turned out to be extremely close. Some possible reasons that the plots in Figure do not exactly match up could be: the resolution of the PMT; the approximate equation did not give an exact correlation to the count rate, which means that the energy spectrum in not perfect; the approximation of the energy loss could be wrong.

Efficiency:

To compare the results of this report with the results of a similar efficiency report done by Matt Schwab for his senior thesis, his efficiency for a similar SSD threshold was above 95%. The efficiency ND SSDs was well also above 95%, and from these results it is safe to conclude that the Silicon Strip Detectors are extremely efficient in detecting charged and uncharged particles.

The error turned out to be reasonable. During earlier runs of the experiment the time scale was around ten minutes and the error was not so good. The longer time scale of one and a half hours reduced the error to an acceptable value.

During this experiment I have become aware of how useful the PMT is in particle detection experiments. From the experienced I gained during this experiment I have been asked to setup a muon lifetime experiment this summer. Overall I would regard my experiences with the PMT has successful, and I have become generally knowledgeable about the use of Scintillation counters in experimentation.

In closing, I must say that this experiment was a success on many levels. The achievement of determining the Energy Spectrum of the beta particles and mating it with theoretical predictions is very exciting. Accomplishing the energy spectrum required many of the topics that were taught to me at UCSC.

The efficiency of the SSD was the result that gave me confidence that I could conduct an important research experiment and see it to a triumphant end. This was very important to me because I came to UCSC to gain experience in performing research experiments, at the culmination of this report I have a feeling that I chosen a career that will excite me and continue to keep happy.

Acknowledgments:

I would like to begin by offering by deepest thanks to Hartmut Sadrozinski for helping me all along the way and offering opportunities I never imagined possible. Many thanks to Marcus Ziegler for answering all the questions I had and for the endless help in my pursuit of knowledge. I would also like to thank David Thayer for helping me with all the little tricks that make a good machinist. Deep thanks to my friends and colleagues at SCIPP: Max Wilder, Ned Spencer, and Jason Heimann for your generous help.

To my wife Patricia, my son Logan, and Susan thank you so very much for your understanding and support.

References:

[1] National Institute for Standards and Technology ESTAR website, April 1, 2004, http://physics.nist.gov/PhysRefData/Star/Text/ESTAR.html

[2] Kieran Maher, "DEXA: Radiation Safety Scintillation Counters" web page; March 6, 2004, www.bh.rmit.edu.au/mrs/DigitalRadiography/DRPapers/DEXA_ScintDetectors.html

[3] SCIONIX, "General" web page; March 8, 2004, www.scionixusa.com/general.html

[4] Brian Keeney, "A Silicon Telescope for Applications in Nanodosimetry," UCSC Physics senior thesis, June 2002

[5] Hartmut Sadrozinski, "Applications of Silicon Detectors," UCSC Scipp 2000

[6] Brian Keeney, "A Silicon Telescope for Nanodosimetry in Biomedical Applications," UCSC Scipp, Novemeber 2002

[7] The European Physical Journal, "Review of Particle Physics," vol.15 num 1-4 2000

[8] Donald H. Perkins, "Introduction to High Energy Physics," Fourth Edition, 2000

[9] Hartmut Sadrozinski, Personal Interview, January-May 2004

Appendix:

Appendix A1:
ND Efficiency Hardware setup:

Close up of the spatial relationship between the scintillator and SSD module.

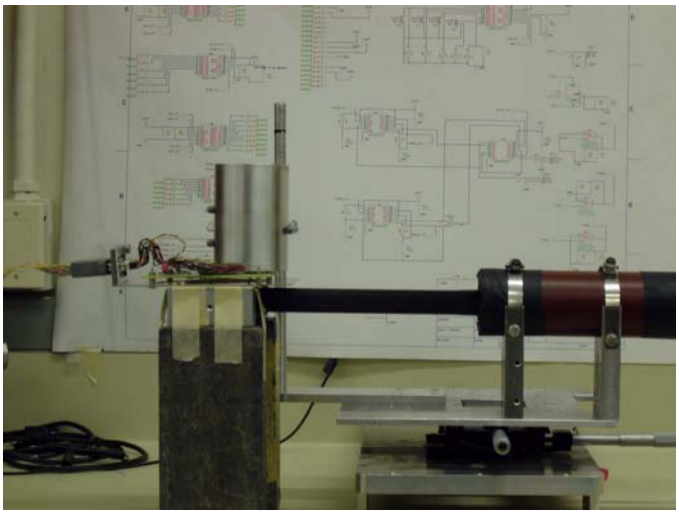

The ND efficiency setup without the light box.

The ND efficiency setup with light box, decorated!

The data acquisition computer and ND setup with light box

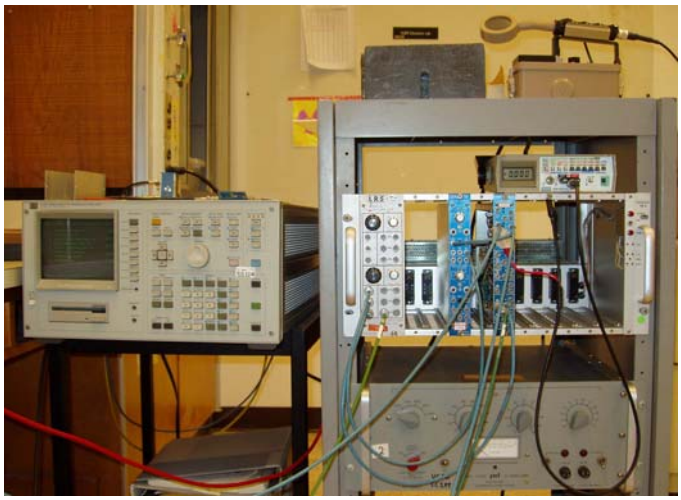

Semiconductor parameter analyzer, for SSD and rack electronics for PMT and efficiency.

Appendix A2:

Mechanical Drawings of Collimator:

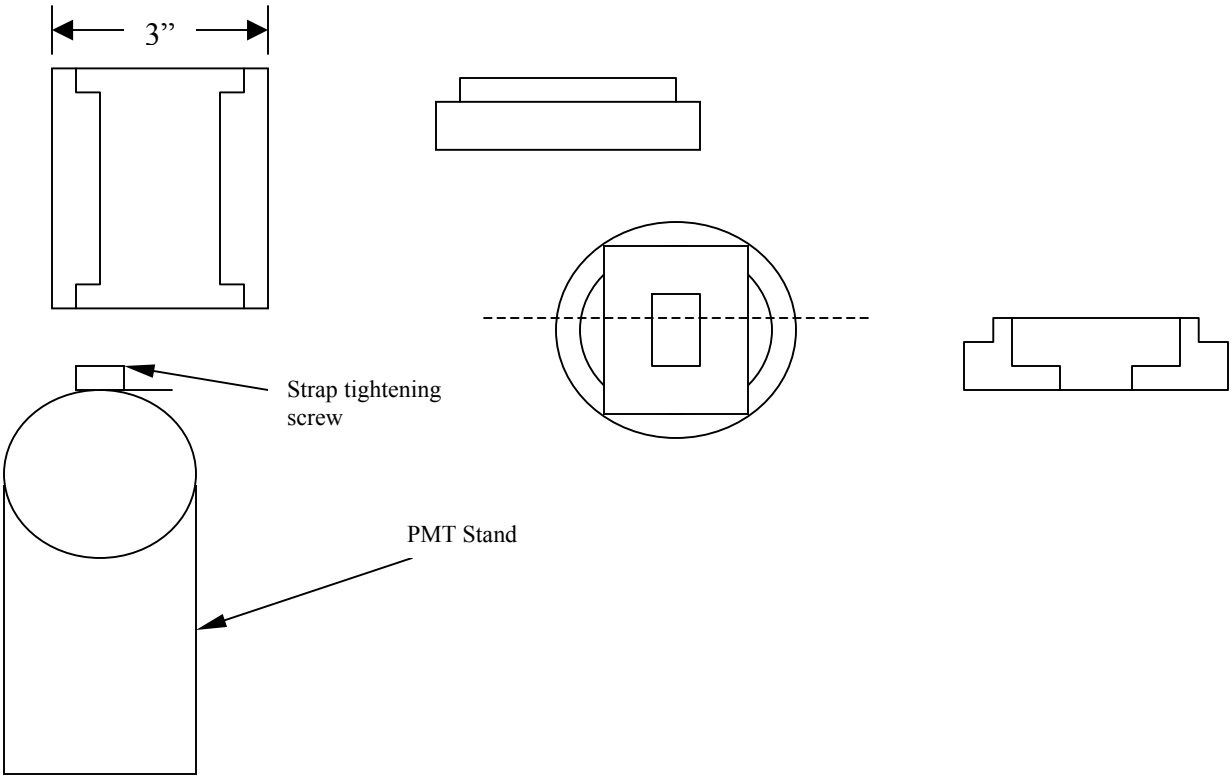

Appendix A3:

Visual Basic Code:
This is the code that reads out the count rates from the frequency generator to an Excel spreadsheet. The program has fields for input voltage, threshold voltage, and time scale.

```
Dim xlApp As Excel.Application
Dim xlBook As Excel.Workbook
Dim xlSheet As Excel.Worksheet
Dim iRow As Integer
Dim iCol As Integer

Const MAX_COLS As Integer = 256

Private Sub Command1_Click()
    If txtBias.Text = "0" Then
        MsgBox "Enter a bias voltage, John!"
    ElseIf txtThreshold.Text = "0" Then
        MsgBox "Enter a threshold, John!"
    ElseIf (Not IsNumeric(txtCount.Text)) Then
        MsgBox "That's an invalid count period, John!"
    Else
        Dim countlength As Double
        Dim count As Double
        Dim rate As Single

        countlength = val(txtCount.Text)
        count = 0
        iCol = 5

        If (countlength / 10) > (MAX_COLS - 3) Then
            MsgBox "That count period is too long, John!"
        Else
            xlSheet.Cells(iRow, 1).value = txtBias.Text
            xlSheet.Cells(iRow, 2).value = txtThreshold.Text
            xlSheet.Cells(iRow, 4).value = txtCount.Text

            While ((count < countlength) And (iCol <
MAX_COLS))
                rate = ct_getcount()
                count = count + 10
                xlSheet.Cells(iRow, iCol).value = rate
                iCol = iCol + 1
            Wend

            xlSheet.Cells(iRow, 3).value =
"=average(RC[2]:RC[253])"
            iRow = iRow + 1
        End If
    End If
End Sub

Private Sub Form_Load()
```

```
    Set xlApp = CreateObject("Excel.Application")
    xlApp.WindowState = xlMinimized
    xlApp.Visible = True
    Set xlBook = xlApp.Workbooks.Add
    Set xlSheet = xlBook.Worksheets(1)

    Call ct_init

    With xlSheet
        .Cells(1, 1).value = "Bias voltage"
        .Cells(1, 2).value = "Threshold"
        .Cells(1, 3).value = "Average rate"
        .Cells(1, 4).value = "Count period"
        .Cells(1, 5).value = "Rates..."
        .Cells(2, 1).value = "(V)"
        .Cells(2, 2).value = "(mV)"
        .Cells(2, 3).value = "(Hz)"
        .Cells(2, 4).value = "(S)"
        .Cells(2, 5).value = "(Hz)"
    End With
    iRow = 3
    iCol = 1
End Sub

Private Sub Form_Unload(Cancel As Integer)
    Call ct_release
    If iCol = 1 Then
        xlBook.Saved = True
        xlApp.Quit
    End If
    Set xlApp = Nothing
End Sub
```